# INVESTIGATION OF ENZYME SELECTIVITY IN THE HUMAN CYP2C SUBFAMILY: HOMOLOGY MODELLING OF CYP2C8, CYP2C9 AND CYP2C19 FROM THE CYP2C5 CRYSTALLOGRAPHIC TEMPLATE

David F.V. Lewis[1,*], Maurice Dickins[2], Brian G. Lake[3] and Peter S. Goldfarb[1]

[1]*School of Biomedical and Molecular Sciences, University of Surrey, Guildford, Surrey,*
[2]*Pfizer Central Research, Ramsgate Road, Sandwich, Kent and*
[3]*BIBRA International Limited, Woodmansterne Road, Carshalton, Surrey, UK*

**SUMMARY**

Homology modelling of human CYP2C subfamily enzymes, CYP2C8, CYP2C9 and CYP2C19, based on the rabbit CYP2C5 crystal structure template is reported. The relatively high sequence homologies (75-80%) between the rabbit CYP2C5 and human CYP2C subfamily enzymes tend to indicate that the resulting structures should prove adequate models of these major catalysts of human drug metabolism. Selective substrates of all three human CYP2C enzymes are found to fit closely within the putative active sites in a manner which is consistent with site-directed mutagenesis experiments and known positions of substrate metabolism. The specific interactions between substrates and enzymes can be used to rationalize the variation in substrate binding affinity and generate QSAR models for both inhibition and metabolism via CYP2C family enzymes, yielding a generally good agreement with experimental binding data obtained

* Author for correspondence:
David F.V. Lewis
School of Biomedical and Molecular Sciences
University of Surrey
Guildford, Surrey, GU2 7XH, UK
e-mail: d.lewis@surrey.ac.uk

from $K_m$ values, with correlation coefficients (R values) of between 0.97 and 0.99 depending on the QSAR equation produced.

**KEY WORDS**

cytochrome P450, xenobiotic metabolism and activation, human CYP2C, homology modelling, CYP2C5 structural template

## INTRODUCTION

The cytochromes P450 (CYP) constitute a superfamily of haem-thiolate enzymes of which over 2,000 individual members are known, encompassing many species and spanning all five biological kingdoms /1-4/. P450s from families CYP1, CYP2 and CYP3 are associated with the Phase 1 metabolism /5/ of the majority of drug substrates in *Homo sapiens*, where P450-catalyzed drug oxidations account for about 80% of all drug metabolism in man /6/. Of this, approximately 40% of human P450-dependent drug metabolism is mediated via polymorphic enzymes /7/. Enzymes of the CYP2 family are of great importance in the Phase 1 metabolism of pharmaceutical agents, and include several polymorphically-expressed P450s, such as CYP2D6 and CYP2C19. The CYP2C subfamily in humans /8/ comprises three enzymes, CYP2C8, CYP2C9 and CYP2C19 /9/, which in total account for about 20% of the total P450 complement and catalyse around 24% of all P450-mediated metabolism of drug substrates /5/. Of these three enzymes, CYP2C9 represents the major form and, although there is some evidence for allelic variants in CYP2C9, it is CYP2C19 which has been more closely associated with polymorphisms in human drug metabolism /6,7/. We have shown previously that the CYP2C5 crystal structure /10/ represents a satisfactory template for the homology modelling of human CYP2 family enzymes /11,12/. In a previous study /13/ we reported homology modelling of CYP2C9 and CYP2C19 enzymes from the CYP102 structure. Consequently, it is of interest to investigate the feasibility of using the CYP2C5 template for rationalizing the metabolism of a significant number of compounds which act as substrates for CYP2C8, CYP2C9 or CYP2C19.

The current work constitutes a homology modelling study of the human CYP2C subfamily enzymes and their selective substrates using CYP2C5 as a crystallographic template structure. Table 1 provides details of some selective substrates and inhibitors for these enzymes, including physicochemical properties /14,15/. Information on structural determinants of substrate specificity have been reported in the literature /16-23/, and Table 2 indicates the routes of metabolism for a number of selective substrates /24-52/.

## METHODS

An alignment between a number of CYP2 family enzymes, including that of the CYP2C5 crystal structure used as a template for homology modelling of other CYP2C subfamily enzymes in this study, has been reported previously /11/. There is a high sequence identity between CYP2C5 and CYP2C8 (76%), CYP2C9 (78%) and CYP2C19 (77%), as would be expected for P450s within the same subfamily. Using the Sybyl Biopolymer module (Tripos Associates, St. Louis, MO, USA) each human CYP2C enzyme was constructed from the CYP2C5 template (pdb code: ldt6) by residue replacement as required by the alignment shown previously*. No deletions were necessary but a small stretch of peptide three residues in length was inserted within the H-I loop region in each case, and this was modelled via pdb loop search routines within the Sybyl Biopolymer package. Following generation of the raw models, each structure was energy minimised using molecular mechanics (Tripos force field) to achieve low energy geometries which satisfied the conformational requirements for protein structures in terms of backbone and side-chain bond lengths, bond angles and torsional angles. Once minimum energy geometries had been obtained, each CYP2C structure was probed using selective substrates and inhibitors. This process was facilitated by the position of the progesterone substrate in CYP2C5 /10/, and from site-directed mutagenesis evidence on amino acid residues which affect the binding and metabolism of CYP2C substrates. All molecular modelling studies were conducted on a Silicon Graphics Indigo$^2$ 10000 High Impact graphics workstation operating under UNIX.

* See Figure 1 on page 99 /75/ or page 118 /76/ in this volume.

## RESULTS AND DISCUSSION

Table 1A-C provides information on several known substrates of CYP2C8, CYP2C9 and CYP2C19, respectively, obtained from the literature, with details on metabolism summarized in Table 2. The structures of each human CYP2C enzyme minimised smoothly over 100 iterative cycles of molecular mechanics, displaying final energies of -1246.3, -1239.5 and -1269.5 kcal.mol$^{-1}$ for CYP2C8, CYP2C9 and CYP2C19, respectively. The results of substrate probes on each of the three P450s are now discussed under individual subheadings for each CYP2C enzyme.

### 1. CYP2C8 model

The putative active site of CYP2C8 is shown in Figure 1, where the bound selective substrate, rosiglitazone, is orientated for *N*-demethylation via several favourable contacts with complementary amino acid residues. The distance between one of the *N*-methyl hydrogen atoms and the haem iron is 4.96 Å for the docked interaction presented in Figure 1, in which a combination of hydrogen bonding to asparagine-99 and serine-114 via the substrate's thiazolidinone ring and $\pi$-$\pi$ stacking with phenylalanine-205, together with hydrophobic contacts to isoleucine-113, alanine-297, valine-366 and valine-477, serve to assist cooperatively in orientating the rosiglitazone molecule such that the *N*-methyl group is positioned directly above the haem iron atom (some residues have been omitted for clarity). Other selective substrates, such as retinoic acid, taxol and cerivastatin, all fit within the CYP2C8 active site in a similar manner to that of rosiglitazone, and the inhibitor, sulfinpyrazone, is also able to occupy the CYP2C8 haem environment in an analogous fashion to those exhibited by selective substrates of this enzyme. Although the active site residues mentioned above have not been probed via site-directed mutagenesis of CYP2C8, the majority have been investigated in other CYP2C subfamily enzymes, and this information is summarized in Table 3 /16-19,53-74/.

The characteristics of typical CYP2C8 substrates are listed in Table 1A, although it should be recognized that some of these are also metabolised by other P450s, and some of which involve different sites of metabolism. In general, CYP2C8 substrates are either neutral or weakly acidic in character, and dissociation at physiological pH can

**TABLE 1A**

Characteristics of CYP2C8 substrates

| Compound | log P | $pK_a$ | log $D_{7.4}$ | $M_r$ | $K_m$ (μM) | $\Delta G_{bind}$ (kcal.mol$^{-1}$) |
|---|---|---|---|---|---|---|
| **Arachidonic acid** | 6.98 | 4.5[a] | 4.08 | 304.46 | 20.5 | -6 6501 |
| **Carbamazepine*** | 2.28 | neutral | 2.28 | 236.27 | N/A | N/A |
| **Cerivastatin*** | 4.54[c] | 4.32[a] | 0 61[c] | 459.55 | N/A | N/A |
| **Diclofenac†** | 4.40 | 4.22[a] | 1.13 | 296.15 | 630 | -4.5400 |
| **Retinoic acid** | 6.58[c] | 5.12[a] | 4.31[c] | 300 44 | 9 | -7.1572 |
| **Retinol** | 6.33[c] | neutral | 6.33[c] | 286.50 | N/A | N/A |
| **Rosiglitazone** | 2.43[c] | 6.4[a] | 2.02[c] | 357.46 | 10 | -7.0923 |
| **Taxol*** | 2.28 | neutral | 2.28 | 853.92 | 5 | -7.5193 |
| **Trimethoprim*** | 0 67 | 6.2[b] | 0.64 | 290.32 | N/A | N/A |
| **Zopiclone** | -0.36[c] | 9.41[b] | -2.29[c] | 388.81 | 71 | -5.8848 |

a = acidic; b = basic; c = calculated value (Pallas Software, CompuDrug Limited, Budapest).
N/A = data not available.
* also a CYP3A4 substrate; † also a CYP2C9 substrate.
References to physicochemical data: /14,15/.

**TABLE 1B**

Characteristics of CYP2C9 substrates

| Compound | log P | $pK_a$ | log $D_{7.4}$ | $M_r$ | $K_m$ (μM) | $\Delta G_{bind}$ (kcal.mol$^{-1}$) |
|---|---|---|---|---|---|---|
| **Phenytoin** | 2.37 | 8.1[a] | 2.39 | 252.27 | 45 | -6.1658 |
| **Tolbutamide** | 2.34 | 5.43[a] | 0.37 | 270.35 | 132 | -5.5028 |
| **S-Ibuprofen** | 3.51 | 5.2[a] | 1.31 | 206.28 | 52 | -6.0767 |
| **Diclofenac** | 4.40 | 4.22[a] | 1.22 | 296.15 | 6 | -7.4070 |
| **S-Warfarin** | 2.52 | 5.1[a] | 0.12 | 308.33 | 4 | -7.6568 |
| **Tienilic acid** | 3.15[c] | 4.8[a] | 0.55[c] | 331.17 | 6 | -7.4070 |
| **58C80** | 5.18[c] | 5.0[a] | 2.78[c] | 312.44 | 141 | -5.4622 |
| **S-Naproxen** | 3.18 | 4.15[a] | 0.33 | 230.26 | 126 | -5.5315 |
| **Piroxicam** | 1.58 | 6.3[a] | 0.45 | 331.34 | 40 | -6.2383 |
| **Mefenamic acid** | 5.12 | 4.2[a] | 2.00 | 241.29 | 7 | -7.6568 |

58C80 = 2-(4-t-butylcyclohexyl)-3-hydroxy-1,4-naphthoquinone; a = acidic; c = calculated values (Pallas Software Compu-Drug Limited, Budapest); log P = logarithm of the octanol-water partition coefficient, P; $pK_a$ = negative logarithm of the dissociation constant, $K_a$; log $D_{74}$ = logarithm of the distribution coefficient, D, at pH 7.4; $M_r$ = relative molecular mass; $K_m$ = Michaelis constant for substrate metabolism (μM); $\Delta G_{bind} = RT\ln K_D$ where $K_D$ is the substrate dissociation constant (μM), R is the gas constant and T is the absolute temperature.
References to physicochemical data: /14,15/.

**TABLE 1C**

Characteristics of CYP2C19 substrates

| Compound | log P | $pK_a$ | log $D_{7.4}$ | $M_r$ | $K_i$ (μM) | $pK_i$ | $K_m$ (μM) | $\Delta G_{bind}$ (kcal.mol$^{-1}$) |
|---|---|---|---|---|---|---|---|---|
| Hexobarbital | 1.49 | 8.2[b] | 0.63 | 236.37 | N/A | N/A | 740 | -4.4409 |
| Moclobemide | 2.13 | 7.09[b] | 1.96 | 268.77 | N/A | N/A | N/A | N/A |
| R-Mephobarbital | 1.86 | 7.8[b] | 1.31 | 246.26 | N/A | N/A | N/A | N/A |
| S-Mephenytoin | 1.74[c] | 8.1[b] | 0.96[c] | 218.28 | 60 | 4.2218 | 38 | -6.2699 |
| Omeprazole | 2.23 | 8.7[b] | 0.91 | 345.45 | 4.1 | 5.3832 | 8.6 | -7.1852 |
| Proguanil | 2.53 | 10.6[b] | -0.47 | 253.73 | N/A | N/A | 96 | -5.6990 |
| Propranolol | 3.37 | 9.5[b] | 1.18 | 259.35 | 112 | 3.9508 | N/A | N/A |
| Diazepam | 2.84 | 4.75[b] | 2.86 | 284.74 | 100 | 4.0000 | 20 | -6.6653 |
| R-Warfarin | 2.52 | 5.1[a] | 0.22 | 308.33 | 32 | 4.4948 | 60 | -5.9885 |
| Phenytoin | 2.47 | 8.1[a] | 2.44 | 252.27 | 280 | 3.5528 | 70 | -5.8936 |
| LY307640 | 1.79[c] | 5.4[b] | 1.79[c] | 359.48 | 9.2 | 5.0362 | 19 | -6.6969 |
| Fluconazole[I] | 0.50 | 2.03[b] | -1.43[c] | 306.30 | 2 | 5.6990 | – | – |

LY307640 = 2-[[[4-(3-methoxypropoxy)-3-methyl-2-pyridinyl]methyl]sulfinyl]-1H-benzimidazole (also known as paripazole).
a = acidic; b = basic; c = calculated value (Pallas Software, CompuDrug Limited, Budapest).
I = inhibitor (and does not act as a substrate); $K_m$ = Michaelis constant (μM) for substrate metabolism;
$K_i$ = inhibition constant for substrate metabolism; N/A = data not available.
References to physicochemical data /14,15/

**TABLE 2**

Distances between sites of metabolism and haem iron for human CYP2C substrates

| Compound | Route of Metabolism | Reference | Distance (Å) |
|---|---|---|---|
| **A. CYP2C8 Substrates** | | | |
| Rosiglitazone | N-demethylation | /24/ | 4.096 |
| Retinoic acid | 4-hydroxylation | /29-31/ | 2.757 |
| Taxol | 6α-hydroxylation | /32/ | 2.369 |
| Carbamazepine | 10,11-epoxidation | /33/ | 7.073 |
| Zopiclone | N-demethylation | /34/ | 2.459 |
| Chloromethyldiethoxyfluorescein | O-deethylation | /35/ | 3.844 |
| Cerivastatin | O-demethylation | /36/ | 5.075 |
| Trimethoprim | O-demethylation | /5/ | 4.359 |
| Zidovudine | azide reduction | /5/ | 4.286 |
| Amiodarone | N-deethylation | /37/ | 3.615 |
| **B. CYP2C9 Substrates** | | | |
| Diclofenac | 4′-hydroxylation | /25/ | 6.484 |
| Tolbutamide | 4-methyl hydroxylation | /25/ | 5.749 |
| Tienilic acid | S-oxidation | /25/ | 3.273 |

| | | | |
|---|---|---|---|
| S-Warfarin | 7-hydroxylation | /25/ | 6.284 |
| Ibuprofen | isobutyl oxidation | /25/ | 4.055 |
| Mefenamic acid | 3′-methyl hydroxylation | /38/ | 7.284 |
| Naproxen | O-demethylation | /39/ | 3.341 |
| 58C80 | tertiary butyl oxidation | /25,40/ | 5.800 |
| Piroxicam | 5′-hydroxylation | /41/ | 6.195 |
| Losartan | hydroxymethyl oxidation | /42/ | 6.206 |
| **C. CYP2C19 Substrates** | | | |
| Omeprazole | 5-methyl hydroxylation | /43/ | 4.959 |
| S-mephenytoin | 4-hydroxylation | /44/ | 5.755 |
| Proguanil | isopropyl oxidation | /45/ | 5.045 |
| Diazepam | N-demethylation | /46/ | 7.279 |
| Phenytoin | 4′-hydroxylation | /47/ | 6.535 |
| Hexobarbital | 3′-hydroxylation | /48/ | 6.987 |
| Mephobarbital | 4-hydroxylation | /49/ | 5.983 |
| Moclobemide | morpholine ring oxidation | /50/ | 6.440 |
| Melatonin | O-demethylation | /51/ | 3.697 |
| LY307640 | O-demethylation | /52/ | |

**TABLE 3**

Site-directed mutagenesis and allelic variants in the CYP2C subfamily

| CYP | Change | 2C5 | SRS | Region/comments | References |
|---|---|---|---|---|---|
| 2C11 | P30A | P30 | – | polyproline motif | /53,54/ |
| 2C11 | P33A | P33 | – | polyproline motif | /53,54/ |
| 2C11 | P35A | P35 | – | polyproline motif | /53,54/ |
| 2C11 | P37A | P37 | – | polyproline motif | /53,54/ |
| 2C9 | R97A | T97 | 1 | B-C loop | /55/ |
| 2C9 | I99H | S99 | 1 | B-C loop: substrate interaction | /19/ |
| 2C9 | L102A | I102 | 1 | B-C loop: substrate interaction | /55/ |
| 2C9 | R105A | K105 | 1 | B-C loop | /55/ |
| 2C2 | G111V | G111 | 1 | B-C loop | /56/ |
| 2C2 | I113C | A113 | 1 | B-C loop: substrate interaction | /56,57/ |
| 2C2, 2C9 | F114L | F114 | 1 | B-C loop: substrate interaction | /56,16,58/ |
| 2C2 | S115R | S115 | 1 | B-C loop | /56/ |
| 2C2 | G117V | A117 | – | B-C loop | /56,59/ |
| 2C2 | W120L | W120 | – | C helix: conserved tryptophan | /56/ |
| 2C9 | R144C | R144 | – | D helix: reductase interaction | /58,60/ |
| 2C3 | I178M | I178 | – | E helix: contact with I helix | /61/ |
| 2C19 | S180C | S180 | – | E helix: close to R144 position | /62/ |
| 2C9 | S220P | P220 | – | F-G loop | /19/ |

| | | | | | |
|---|---|---|---|---|---|
| 2C9 | P221T | A221 | – | F-G loop | /19/ |
| 2C9 | E241K | K241 | – | G helix | /63/ |
| 2C9 | E274- | E274 | – | H-I loop | /64/ |
| 2C9 | K275- | N275 | – | H-I loop | /64/ |
| 2C9 | N286S | S283 | – | I helix | /63,65/ |
| 2C9 | I289N | I286 | – | I helix | /63 65/ |
| 2C14 | T301S | T298 | 4 | I helix: conserved distal threonine | /66/ |
| 2C9 | Y358C | F355 | – | K helix | /60/ |
| 2C9 | I359L | I356 | – | K helix | /17,18/ |
| 2C3 | S364T | N362 | 5 | $\beta_1$(4) sheet | /57,61/ |
| 2C9 | L362A | L363 | 5 | $\beta_1$(4) sheet | /69/ |
| 2C1 | H368R | H365 | 5 | $\beta_1$(4) sheet: haem propionate interaction | /70/ |
| 2C1 | T369A | T366 | 5 | $\beta_1$(4) sheet | /70/ |
| 2C1 | L374V | V371 | – | $\beta_2$(1) sheet | /70/ |
| 2C1 | D386A | D383 | – | $\beta_1$(3) sheet: close to reductase site | /70/ |
| 2C1 | L388I | I385 | – | $\beta_1$(3) sheet | /70/ |
| 2C9 | G417D | G414 | – | $F_1$ helix | /60,71/ |
| 2C2 | S473V | V470 | 6 | $\beta_4$(2) sheet: substrate interaction | /72/ |
| 2C2 | P480A | P477 | – | $\beta_3$(2) sheet: close to active site | /72/ |
| 2C2 | P481T | P478 | – | $\beta_3$(2) sheet: close to active site | /72/ |

SRS = substrate recognition site /74/. Review references: /2,21,22,13,73/.

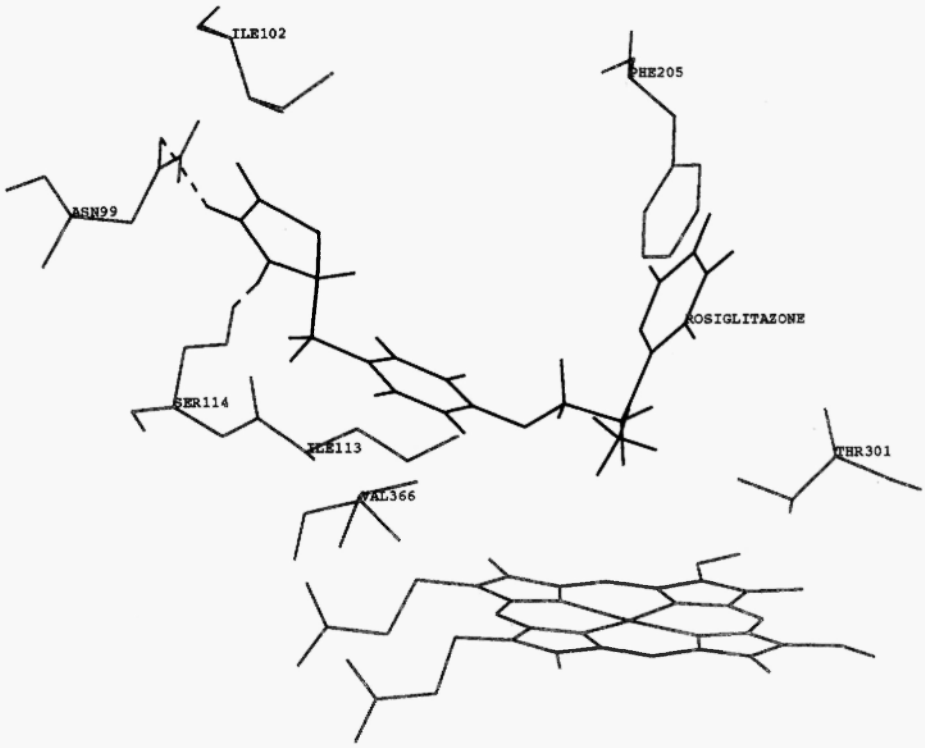


**Fig. 1:** Rosiglitazone is shown orientated within the putative active site of CYP2C8 where a combination of hydrogen bonding and π-π stacking interactions positions the substrate for *N*-demethylation. Hydrogen bonds are depicted as dashed lines.

have a marked effect on their overall lipophilic nature. Although there is some degree of overlapping selectivity with CYP2C9, the substrates of CYP2C8 generally tend to possess relatively larger sized molecules than those of CYP2C9, possibly reflecting the respective active site dimensions and topography of the two enzymes. In addition, the molecular conformation of some typical CYP2C8 substrates tends to be that of an elongated S-shape, as exemplified by rosiglitazone (see Fig. 1). Moreover, it is found that the carboxyl groups of certain CYP2C8 substrates, such as retinoic acid, arachidonic acid and cerivastatin, are superimposible within the active site and, furthermore, overlay with the weakly acidic thiazolidinone ring of rosiglitaz-

one where they also make analogous contacts with complementary amino acid residues in the CYP2C8 haem pocket. In terms of distances between sites of metabolism and hydrogen bond contacts, there is a general rule of 12 governing the number of intervening heavy atoms, as evidenced by inspection of the structures of rosiglitazone, retinoic acid, taxol, zopiclone and zidovudine (AZT).

## 2. CYP2C9 model

The putative site of CYP2C9 is presented in Figure 2, which shows how the selective substrate, diclofenac, may orientate within the haem locus for 4-hydroxylation; this is facilitated by favourable contacts with a number of complementary amino acid residues. In particular, phenylalanine-114 and phenylalanine-476 form π-π stacking interactions with aromatic groups in the substrate molecule, and there is also a hydrogen bond formed with glutamine-214. Hydrophobic contacts between diclofenac and the CYP2C9 active site include residues isoleucine-99, isoleucine-205 and leucine-208, whereas isoleucine-362, leucine-102 and leucine-366 are also relatively close to the substrate molecule, although some of these residues have been omitted for clarity in Figure 2. There is direct evidence from site-specific mutation experiments /16/ that phenylalanine-114 is responsible for aromatic π-π stacking with another CYP2C9 substrate, warfarin, and the change I359L alters both regio- and stereoselectivity of warfarin metabolism /17,18/. Moreover, glutamine-214 is close to a pair of residues which appear to affect omeprazole binding in the CYP2C19 orthologue /19/. Furthermore, the residue at position 99 appears to be of importance in explaining altered substrate selectivities between CYP2C9 and CYP2C19 /19,20/. In the orientation shown in Figure 2, the 4-hydrogen position on the substrate lies at a distance of 6.48 Å from the haem iron, and this represents the closest hydrogen atom on diclofenac to the iron atom. Other typical CYP2C9 substrates tend to lie somewhat closer to the haem, however. The 4-methyl hydrogen of tolbutamide, for example, is 5.75 Å from the haem iron, and the isobutyl hydrogen of *S*-ibuprofen which is closest to the haem iron lies at a distance of 4.06 Å. For a superimposed template of typical CYP2C9 substrates (totalling seven compounds) docked within the putative active site, the hydrogen to iron distances for the sites of metabolism range from 3.27 Å (tienilic acid) to 7.28 Å (mefenamic

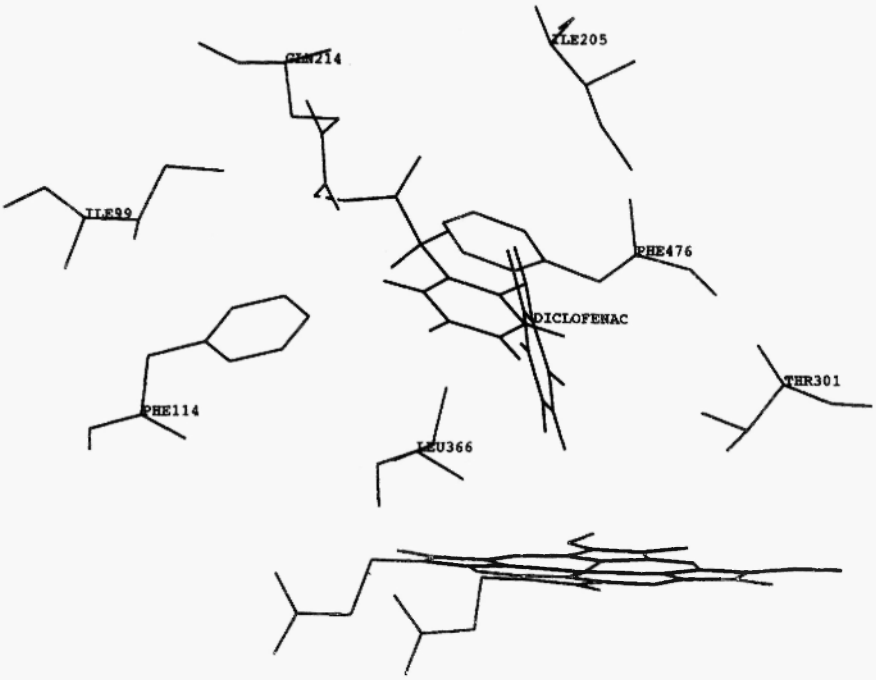


**Fig. 2:** Diclofenac is shown within the putative active site of CYP2C9 where a combination of hydrogen-bonded and π-π stacking interactions orientates the substrate for 4-hydroxylation. Hydrogen bonds are presented as dashed lines.

acid) and the average distance is 5.47 Å, which is close to the corresponding distance (5.66 Å) between the 4-amino group and the haem iron of the selective CYP2C9 inhibitor, sulfaphenazole /23/. In general, the more selective substrates of CYP2C9 can be overlaid within the putative active site such that their known positions of metabolism lie closest to the haem iron and where the molecules also make analogous contacts with nearby amino acid residues, many of which have been probed using site-directed mutagenesis (see Table 3 for a summary).

Many CYP2C9 substrates are weakly acidic in character, with $pK_a$ values lying within the range between 4.1 and 6.3 $pK_a$ units, although phenytoin is very weakly acidic with a $pK_a$ of 8.1 (see Table 1B). This

physicochemical characteristic appears to have importance in explaining the variation in binding affinity for CYP2C9 substrates, as discussed in Section 4, and it is possible to use this weakly acidic character of most CYP2C9 substrates as a means of differentiating from those of other P450 enzymes /21/.

### 3. CYP2C19 model

In contrast, most CYP2C19 substrates are weakly basic compounds, but both phenytoin and R-warfarin are exceptions by displaying a weak acidic character (see Table 1C). Figure 3 shows the putative active site of CYP2C19 with the selective substrate, omeprazole, orientated for 5′-methyl hydroxylation. This position is consistent with available evidence from site-specific mutation data

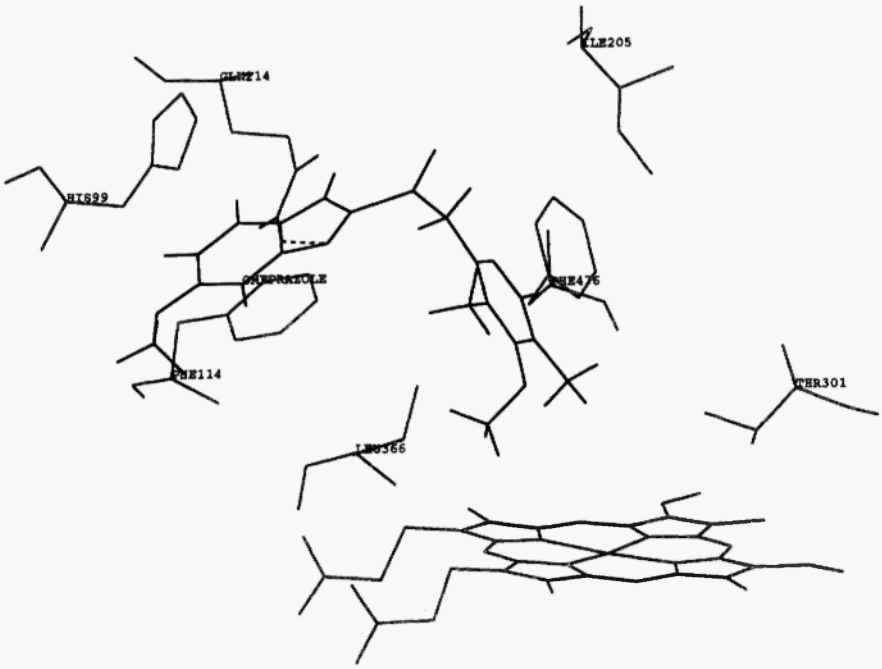


**Fig. 3:** Omeprazole is orientated within the CYP2C19 active site for 5′-methyl hydroxylation via a combination of hydrogen bond and π-π stacked interactions with complementary amino acid residues. Hydrogen bonds are shown as dashed lines.

/16,19/ and it appears that a combination of π-π stacking and hydrogen bond interactions brings about an orientation of omeprazole in the CYP2C19 active site which involves bringing the 5′-methyl group to within 5 Å of the haem iron (actually, 4.96 Å). *S*-Mephenytoin is another example of a selective marker substrate for CYP2C19 and, in this case, the site of metabolism (4′-position) lies at a distance of 5.76 Å from the haem iron atom. These two molecules are largely superimposible within the CYP2C19 active site, making similar contacts with complementary amino acid residues and with overlapping sites of metabolism. In particular, histidine-99 appears to enter into hydrogen bond formation with both omeprazole (Fig. 3) and *S*-mephenytoin. This residue has been the subject of site-directed mutagenesis experiments in CYP2C19 itself, where the change H99I has a marked effect on omeprazole metabolism /19/. Furthermore, phenylalanine-114 is involved in π-π stacking with most CYP2C19 substrates and this residue has been mutated in the orthologous CYP2C9 enzyme /16/, as mentioned previously.

A template of seven CYP2C19 substrates, including omeprazole, *S*-mephenytoin, diazepam, proguanil, mephobarbital, hexobarbital and moclobemide, can be shown to fit within the CYP2C19 active site on the basis of their positions of metabolism being close to the haem moiety. This tends to indicate that certain complementary interactions with amino acid residues are common to most CYP2C19 substrates, especially histidine-99 and phenylalanine-114, although glutamine-214 and phenylalanine-476 are also important. Other residues which are required for hydrophobic interactions in most CYP2C19 substrates include isoleucine-205 and valine-208; the former represents a position which has been probed using site-directed mutagenesis in other CYP2 family enzymes (reviewed in /22/). In addition, some substrates form hydrophobic contacts with leucine-102, valine-113 and leucine-366 which line the haem pocket in CYP2C5. Furthermore, the selective CYP2C19 inhibitor, fluconazole, is able to fit closely within the putative active site of the enzyme by making favourable complementary contacts with the same set of amino acid residues that appear to interact with many CYP2C19 substrates. These interactions, which include hydrogen bonding and π-π stacking, position the fluconazole inhibitor within the CYP2C19 active site such that one of the azole ring nitrogens lies at a distance of 4.81 Å from the haem

iron, and in an orientation consistent with Type II binding (i.e. iron ligation via the azole moiety in this case). Consequently, the general picture for CYP2C19 selectivity involves the potential for at least one π-π stacking interaction and two hydrogen bond interactions: this pharmacophore pattern is also consistent with QSAR analysis of CYP2C19 selective compounds, as summarized in the following section.

**4. QSARs within CYP2C substrates and inhibitors**

Tables 4-6 present the results of previous QSAR analyses on substrates of CYP2C8, CYP2C9 and CYP2C19, respectively. All of these show the importance of hydrogen bond descriptors and lipophilicity in the explanation of potency differences for binding to the relevant CYP2C enzyme, and Table 6 indicates that competitive inhibition of CYP2C19 is related to a similar set of descriptors to those governing substrate binding to the enzyme. The important role of lipophilicity is emphasized by the baseline lipophilicity relationships exhibited by CYP2C9 and CYP2C19 substrates, as shown in Table 7, although the numbers of compounds involved are not large. However, the inclusion of additional factors, such as hydrogen bonds, π-π stacking and loss in bond rotational freedom, which accompany substrate binding, provides very good concordances with binding energies for CYP2C8 (R = 0.98), CYP2C9 (R = 0.99) and CYP2C19 (R = 0.98) substrates as demonstrated by the information shown in Table 8. Consequently, it is possible to make satisfactory estimates of the likely binding affinity of human CYP2C subfamily substrates from a consideration of the various contributions to the overall binding interaction, including partitioning energy from the lipophilic component. However, it is important to investigate the mode of substrate binding within the active site in order to provide an estimate of the likely hydrogen bond and π-π stacking energies.

## CONCLUSIONS

The models of human CYP2C subfamily enzymes generated via sequence homology with the CYP2C5 crystal structure exhibit active site characteristics that are consistent with the known substrate

**TABLE 4**

QSAR dataset for CYP2C8 substrates

| Compound | $M_r$ | $N_{HB}^{Site}$ | $N_{\pi-\pi}^{Site}$ | $K_m$ (μM) | $\Delta G_{bind}$ (kcal.mol$^{-1}$) |
|---|---|---|---|---|---|
| **Chloromethyl-6 6′-diethoxyfluorescein** | 436.91 | 2 | 1 | 25 | -5.5279 |
| **Diclofenac** | 296.15 | 2 | 1 | 630 | -4.5400 |
| **Retinoic acid** | 300 44 | 1 | 0 | 9 | -7.1572 |
| **Rosiglitazone** | 357.46 | 1 | 2 | 10 | -7.0923 |
| **Taxol** | 853.92 | 4 | 1 | 12 | -6.9800 |
| **Zopiclone** | 388.81 | 2 | 1 | 71 | -5.8848 |

$M_r$ = relative molecular mass; $N_{HB}^{Site}$ = number of active site hydrogen bonds;
$N_{\pi-\pi}^{Site}$ = number of active site π-π stacking interactions;
$K_m$ = Michaelis constant (μM) for substrate metabolism;
$\Delta G_{bind}$ = $RT\ln K_m$ where R is the gas constant and T is the absolute temperature.

| QSAR Expression | n | s | R | F |
|---|---|---|---|---|
| 1. $\Delta G_{bind}$ = 2.01 $N_{HB}^{Site}$ (±0.33) − 0.12 $M_r$ (±0.002) − 5.10 | 6 | 0.332 | 0.97 | 25.9 |
| 2. $\Delta G_{bind}$ = 2.12 $N_{HB}^{Site}$ (±0.11) − 0.013 $M_r$ (±0.001) − 0.40 $N_{\pi-\pi}^{Site}$ (±0.08) − 5.44 | 6 | 0.112 | 0.99 | 159.4 |

**TABLE 5**

QSAR dataset for CYP2C9 substrates

| Compound | log P | $pK_a$ | log $D_{7.4}$ | $HB_D$ | $K_m$ (μM) | $\Delta G_{bind}$ (kcal.mol$^{-1}$) |
|---|---|---|---|---|---|---|
| **Phenytoin** | 2.47 | 8.1[a] | 2.39 | 2 | 45 | -6.166 |
| **Tolbutamide** | 2.34 | 5.43[a] | 0.37 | 2 | 132 | -5.503 |
| **Ibnprofen** | 3.51 | 5.2[a] | 1.31 | 1 | 53 | -6.065 |
| **Diclofenac** | 4.40 | 4.22[a] | 1.22 | 2 | 6 | -7.407 |
| **S-Warfarin** | 2.52 | 5.1[a] | 0.12 | 1 | 4 | -7.657 |
| **Tienilic acid** | 3.15[c] | 4.8[a] | 0.55[c] | 1 | 6 | -7.407 |
| **58C80** | 5.18[c] | 5.0[a] | 2.78[c] | 1 | 141 | -5.462 |
| **Naproxen** | 3.18 | 4.15[a] | 0.33 | 1 | 126 | -5.531 |

$K_m$ = Michaelis constant (μM) for substrate metabolism;
58C80 = 2-(4-t-butylcyclohexyl)-3-hydroxy-1,4-naphthoquinone;
$HB_D$ = number of hydrogen bond donors in the molecule.

| QSAR Expression | n | s | R | F |
|---|---|---|---|---|
| 1. $\Delta G_{bind}$ = 8.62 log $D_{7.4}$ (±0.82) − 8.02 log P (±0.79) − 6.26 $pK_a$ (±0.62) + 0.57 $HB_D$ (±0.19) + 42.74 | 8 | 0.2267 | 0.99 | 29.5 |

**TABLE 6**

QSAR dataset for CYP2C19 substrates and inhibitors

| Compound | log P | $M_r$ | $HB_D$ | $HB_A$ | $pK_i$ | $K_m$ (μM) | $\Delta G_{bind}$ (kcal.mol$^{-1}$) |
|---|---|---|---|---|---|---|---|
| **S-Mephenytoin** | 1.74 | 218.28 | 1 | 2 | 4.2218 | 38 | -6.2699 |
| **Omeprazole** | 2.23 | 245.45 | 1 | 5 | 5.3872 | 8.6 | -7.1852 |
| **Propranolol** | 3.37 | 259.35 | 2 | 3 | 3.9508 | N.A. | N/A |
| **Diazepam** | 2.84 | 284.74 | 0 | 2 | 4.0000 | 20 | -6.6653 |
| **R-Warfarin** | 2.52 | 308.33 | 1 | 4 | 4.4948 | 60 | -5.9885 |
| **Phenytoin** | 2.47 | 252.27 | 2 | 2 | 3.5528 | 70 | -5.8936 |
| **LY307640** | 1.79 | 359.48 | 1 | 5 | 5.0362 | 19 | -6.6969 |
| **Fluconazole** | 0.50 | 306.30 | 1 | 7 | 5.6990 | N.A. | N/A |
| **Tranylcypromine** | 1.52 | 133.20 | 2 | 1 | 5.0969 | N/A | N/A |
| **Demethyldiazepam** | 3.32 | 270.73 | 1 | 2 | 3.9393 | N/A | N/A |
| **Hexobarbital** | 1.49 | 236.37 | 1 | 3 | N.A. | 740 | -4.4409 |
| **Proguanil** | 2.53 | 253.73 | 5 | 0 | N.A. | 96 | -5.6900 |

$K_i$ = Equilibrium constant (μM) for substrate inhibition; $K_m$ = Michaelis constant (μM) for substrate metabolism; N/A = data not available; $HB_D$ = number of hydrogen bond donors in the molecule; $HB_A$ = number of hydrogen bond acceptors in the molecule

| QSAR Expression | n | s | R | F |
|---|---|---|---|---|
| 1. $pK_i = 0.029\ M_r - 19.13 \log M_r + 0.381\ HB_A - 0.278\ HB_D + 42.094$ (±0.006) (±2.93) (±0.049) (±0.108) | 10 | 0.1720 | 0.98 | 38.4 |
| 2. $\Delta G_{bind} = 198.94 \log M_r - 0.31\ M_r - 2.39 \log P - 399.90$ (±34.71) (±0.05) (±0.39) | 8 | 0.2552 | 0.97 | 23.5 |
| 3. $\Delta G_{bind} = 201.69 \log M_r - 0.31\ M_r - 2.50 \log P + 0.12\ HB_D - 405.68$ (±19.87) (±0.03) (±0.23) (±0.04) | 8 | 0.1460 | 0.99 | 56.2 |

**TABLE 7**

Lipophilicity relationships in CYP2C9 and CYP2C19 substrates

**A. CYP2C9 substrates**

| Compound | log P | $\Delta G_{part}$ | $\Delta G_{bind}$ |
|---|---|---|---|
| **Mefenamic acid** | 5.12 | -7.2625 | -7.3121 |
| **Diclofenac** | 4.40 | -6.2413 | -7.4070 |
| **Ibuprofen** | 3.51 | -4.9788 | -6.0650 |
| **Naproxen** | 3.18 | -4.5107 | -5.5315 |
| **Tolbutamide** | 2.34 | -3.3192 | -5.5028 |

$\Delta G_{bind} = 0.639\ \Delta G_{part} - 3.072$ (±0.124) n = 5; s = 0.3802; R = 0.95; F = 26.5

**B. CYP2C19 substrates**

| Compound | log P | $\Delta G_{part}$ | $\Delta G_{bind}$ |
|---|---|---|---|
| **Diazepam** | 2.84 | -4.0284 | -6.6653 |
| **R-Warfarin** | 2.52 | -3.5745 | -5.9885 |
| **Phenytoin** | 2.47 | -3.5036 | -5.8936 |
| **Prognanil** | 2.53 | -3.5887 | -5.6990 |
| **Hexobarbital** | 1.49 | -2.1135 | -4.4409 |

$\Delta G_{bind} = 1.087\ \Delta G_{part} - 2.083$ (±0.141) n = 5; s = 0.2054; R = 0.98; F = 59.2

$\Delta G_{part} = -RT\ln P$
where R is the gas constant, T is the absolute temperature and
P is the octanol/water partition coefficient.

selectivity of these enzymes. In particular, the derived 3D models of CYP2C8, CYP2C9 and CYP2C19 are consistent with their substrate selectivities, and it is also possible to demonstrate the likely mode of interaction for enzyme inhibitors in each case. The models also exhibit consistency with an extensive body of information from site-directed mutagenesis (summarized in Table 3) structure-activity relationships

**TABLE 8**

Comparison between experimental and calculated $\Delta G_{bind}$ values

**A. CYP2C8 substrates**

| Compound | log P | $\Delta G_{part}$ | $\Delta G_{hb}$ | $\Delta G_{\pi-\pi}$ | $\Delta G_{rot}$ | $\Delta G^{calc}_{bind}$ | $\Delta G^{expt}_{bind}$ |
|---|---|---|---|---|---|---|---|
| **Rosiglitazone** | 2.43 | -3.4469 | -4.0 | -0.9 | 1.2 | -7.1469 | -7.0923 |
| **Retinoic acid** | 6.58 | -9.3335 | -2.0 | 0 | 4.2 | -7.1335 | -7.1572 |
| **Taxol** | 2.28 | -3.2341 | -8.0 | -0.9 | 4.8 | -7.3341 | -7.5193 |
| **Zopiclone** | 0.53 | -0.7518 | -4.0 | -0.9 | 0 | -5.6518 | -5.8848 |
| **Arachidonic acid** | 6.98 | -9.9009 | -2.0 | 0 | 5.4 | -6.5009 | -6.6501 |

**B. CYP2C9 substrates**

| Compound | log P | $\Delta G_{part}$ | $\Delta G_{hb}$ | $\Delta G_{\pi-\pi}$ | $\Delta G_{rot}$ | $\Delta G^{calc}_{bind}$ | $\Delta G^{expt}_{bind}$ |
|---|---|---|---|---|---|---|---|
| **Diclopfenac** | 4.40 | -6.2413 | -2.0 | -0.9 | 1.8 | -7.3413 | -7.4070 |
| **Ibuprofen** | 3.51 | -4.9788 | -2.0 | -0.9 | 1.8 | -6.0788 | -6.0650 |
| **Tienilic acid** | 3.15 | -4.4682 | -4.0 | -0.9 | 1.8 | -7.5682 | -7.4070 |
| **Naproxen** | 3.18 | -4.5107 | -2.0 | -0.9 | 1.8 | -5.6107 | -5.5315 |
| **Tolbutamide** | 2.34 | -3.3192 | -4.0 | -0.9 | 2.4 | -5.6192 | -5.5030 |
| **Mefenamic acid** | 5.12 | -7.2625 | -2.0 | -0.9 | 3.0 | -7.1625 | -7.3121 |
| **S-Warfarin** | 2.52 | -3.5745 | -4.0 | -0.9 | 0.6 | -7.8745 | -7.6570 |
| **Phenytoin** | 2.47 | -3.5036 | -2.0 | -0.9 | 0 | -6.4036 | -6.1660 |

C. CYP2C19 substrates

| Compound | log P | $\Delta G_{part}$ | $\Delta G_{3t}$ | $\Delta G_{\pi\pi}$ | $\Delta G_{10}$ | $\Delta G^{calc}_{bind}$ | $\Delta G^{expt}_{bind}$ |
|---|---|---|---|---|---|---|---|
| **S-Mephenytoin** | 1.74 | -2.4681 | -4.0 | -0.9 | 1.2 | -6.1681 | -6.2699 |
| **Omeprazole** | 2.23 | -3.1632 | -4.0 | -0.9 | 0.6 | -7.4632 | -7.1852 |
| **Hexobarbital** | 1.49 | -2.1135 | -2.0 | -0.9 | 0 6 | -4.4135 | -4.4409 |
| **Proguanil** | 2.53 | -3.5887 | -2.0 | -0.9 | 0.6 | -5.8887 | -5.6990 |
| **Diazepam** | 2.84 | -4.0284 | -2.0 | -0.9 | 0.6 | -6.3284 | -6.6653 |
| **LY307640** | 1.79[c] | -2.5391 | -4.0 | -0.9 | 0.6 | -6.9391 | -6.6969 |
| **R-Mephobarbital** | 1.86 | -2.6383 | -4.0 | 0 | 0.6 | -6.0383 | -5.9392 |

The agreement between experimental and calculated values of $\Delta G_{bind}$ is approximately 98% for the substrates of CYP2C8, CYP2C9 and CYP2C19 shown above.

/23/ and substrate metabolism. Furthermore, QSARs can be generated for substrates of the three human CYP2C subfamily enzymes which enable some degree of rationalization of the contributions to binding affinity, and the role of lipophilicity is emphasized by certain correlations between binding affinity and log P, where P is the octanol-water partition coefficient. However, the inclusion of active site contacts in the form of hydrogen-bonded and $\pi$-$\pi$ stacking interactions is important for deriving satisfactory relationships with experimentally-derived binding affinities for human CYP2C subfamily substrates. It is hoped that this type of approach may be extended to other examples of P450-substrate interactions.

## ACKNOWLEDGEMENTS

The financial support of GlaxoSmithKline Research and Development Limited, Merck Sharp & Dohme Limited and the University of Surrey Foundation Fund is gratefully acknowledged by DFVL.

## REFERENCES

1. Anzenbacher P, Anzenbacherova E. Cytochromes P450 and metabolism of xenobiotics. Cell Mol Life Sci 2001; 58: 737-747.
2. Lewis DFV. Guide to Cytochromes P450 Structure and Function. London: Taylor & Francis, 2001.
3. Nelson DR. Metazoan cytochrome P450 evolution. Comp Biochem Physiol C 1998; 121: 15-22.
4. Lewis DFV. Cytochromes P450: Structure, Function and Mechanism. London: Taylor & Francis, 1996.
5. Rendic S, DiCarlo FJ. Human cytochrome P450 enzymes: a status report summarizing their reactions, substrates, inducers and inhibitors. Drug Metab Rev 1997; 29: 413-580.
6. Evans WE, Relling MV. Pharmacogenomics: translating functional genomics into rational therapies. Science 1999; 286: 487-491.
7. Ingelman-Sundberg M, Oscarson M, McLellan RA. Polymorphic human cytochrome P450 enzymes: an opportunity for individualized drug treatment. Trends Pharmaceut Sci 1999; 20: 342-349.
8. Goldstein JA, de Morais SMF. Biochemistry and molecular biology of the human CYP2C subfamily. Pharmacogenetics 1994; 4: 285-299.

9. Richardson TH, Johnson EF. The CYP2C subfamily. In: Ioannides C, ed. Cytochromes P450 - Metabolic and Toxicological Aspects, Ch 7. Boca Raton, FL: CRC Press, 1996; 161-181.
10. Williams PA, Cosme J, Sridhar V, Johnson EF, McRee DE. Mammalian cytochrome P450 monooxygenase: structural adaptations for membrane binding and functional diversity. Mol Cell 2000; 5: 121-131.
11. Lewis DFV. Homology modelling of human CYP2 family enzymes based on the CYP2C5 crystal structure. Xenobiotica 2002; 32: 305-323.
12. Lewis DFV, Lake BG. Species differences in coumarin metabolism: a molecular modelling evaluation of CYP2A interactions. Xenobiotica 2002; 32: 547-561.
13. Lewis DFV, Dickins M, Weaver RJ, Eddershaw PJ, Goldfarb PS, Tarbit MH. Molecular modelling of human CYP2C subfamily enzymes CYP2C9 and CYP2C19: rationalization of substrate specificity and site-directed mutagenesis experiments in the CYP2C subfamily. Xenobiotica 1998; 28: 235-268.
14. Hansch C, Leo A, Hoekman D. Exploring QSAR: Hydrophobic, Electronic and Steric Constants. Washington, DC: American Chemical Society, 1995.
15. Dollery C. Therapeutic Drugs. Edinburgh: Churchill-Livingstone, 1999.
16. Haining RL, Jones JP, Henne KR, Fisher MB, Koop DR. Enzymatic determinants of the substrate specificity of CYP2C9: role of B-C loop residues in providing the pi-stacking anchor site for warfarin binding. Biochemistry 1999; 38: 3285-3292.
17. Haining RL, Hunter AP, Veronese E, Trager WF, Rettie AE. Allelic variants of human cytochrome P450 2C9: baculovirus-mediated expression, purification, structural characterization, substrate stereoselectivity and prochiral selectivity of the wild-type and I359L mutant forms. Arch Biochem Biophysics. 1996; 333: 447-458.
18. Takanashi K, Tainaka H, Kobayashi K, Yasumori T, Hosekawa M, Chiba K. CYP2C9 $Ile^{359}$ and $Leu^{359}$ variants: enzyme kinetic study with seven substrates. Pharmacogenetics 2000; 10: 95-104.
19. Ibeanu GS, Ghanayem BI, Linko P, Li L, Pedersen LG, Goldstein JA. Identification of residues 99, 220 and 221 of human cytochrome P450 2C19 as key determinants of omeprazole hydroxylase activity. J Biol Chem 1996; 271: 12496-12501.
20. Tsao C-C, Wester MR, Ghanayem B, Coulter SJ, Chanas B, Johnson EF, Goldstein JA. Identification of human CYP2C19 residues that confer S-mephenytoin 4′-hydroxylation activity to CYP2C9. Biochemistry 2001; 40: 1937-1944.
21. Lewis DFV. On the recognition of mammalian microsomal cytochrome P450 substrates and their characteristics. Biochem Pharmacol 2000; 60: 293-306.
22. Lewis DFV. The CYP2 family: models, mutants and interactions. Xenobiotica 1998; 28: 617-661.
23. Smith DA, Jones BC. Speculations on the substrate structure-activity relationship (SSAR) of cytochrome P450 enzymes. Biochem Pharmacol 1992; 44: 2089-2098.

24. Baldwin SJ, Clarke SE, Chenery RJ. Characterization of the cytochrome P450 enzymes involved in the in vitro metabolism of rosiglitazone. Br J Clin Pharmacol 1999; 48: 424-432.
25. Mancy A, Broto P, Dijols S, Dansette PM, Mansuy D. The substrate binding site of human liver cytochrome P450 2C9: an approach using tienilic acid derivatives and molecular modeling. Biochemistry 1995; 34: 10365-10375.
26. He M, Kunze KL, Trager WF. Inhibition of S-warfarin metabolism by sulfinpyrazone and its metabolites. Drug Metab Dispos 1995; 23: 659-663.
27. Miners JO, Birkett DJ. Cytochrome P4502C9: an enzyme of major importance in human drug metabolism, Br J Clin Pharmacol 1998; 45: 525-538.
28. Weinkers LC, Wurden CJ, Storch E, Kunze KL, Rettie AE, Trager WF. Formation of (R)-8-hydroxywarfarin in human liver microsomes. Drug Metab Dispos 1996; 24: 610-614.
29. Marill J, Cresteil T, Lanotte M, Chabot GG. Identification of human cytochrome P450s involved in the formation of all-*trans*-retinoic acid principal metabolites. Mol Pharmacol 2000; 58: 1341-1348.
30. Marill J, Capron CC, Idres N, Chabot GG. Human cytochrome P450s involved in the metabolism of 9-*cis*- and 13-*cis*-retoinoic acids. Biochem Pharmacol 2002; 63: 937-947.
31. Leo MA, Lasker JM, Raucy JL, Kim C-I, Black M, Lieber CS. Metabolism of retinol and retinoic acid by human liver cytochrome P450IIC8. Arch Biochem Biophys 1989; 269: 305-312.
32. Crespi CL, Chang TKH, Waxman DJ. High-performance liquid chromatographic analysis of CYP2C8-catalyzed paclitaxel 6α-hydroxylation. In: Phillips IR, Shephard EA, eds. Cytochrome P450 Protocols. Totowa, NJ: Humana Press, 1998; 123-127.
33. Kerr BM, Thummel KE, Wurden CJ, Klein SM, Kroetz DL, Gonzalez FJ, Levy RH. Human liver carbamazepine metabolism: role of CYP3A4 and CYP2C8 in 10,11-epoxide formation. Biochem Pharmacol 1994; 47: 1969-1979.
34. Becquemont L, Mouajjah S, Escaffre O, Beaune P, Funck-Brentano C, Jaillon P. Cytochrome P450 3A4 and 2C8 are involved in zopiclone metabolism. Drug Metab Dispos 1999; 27: 1068-1073.
35. White INH, Green ML, Legg RF. Fluorescence-activated sorting of rat hepatocytes based on their mixed function oxidase activities towards fluorescein. Biochem J 1987; 247: 23-28.
36. Mück W, Ochmana K, Rohde G, Unger S, Kuhlmann J. Influence of erythromycin pre- and co-treatment on single dose pharmacokinetics of the HMG-CoA reductase inhibitor cerivastatin. Eur J Clin Pharmacokinet 1998; 53: 469-473.
37. Ohyama K, Nakajima M, Nakamura S, Shimada N, Yamazaki H, Yokoi T. A significant role of human cytochrome P450 2C8 in amiodarone N-deethylation: an approach to predict the contribution with relative activity factor. Drug Metab Dispos 2000; 28: 1303-1310.

38. Bonnabry P, Leemann T, Dayer P. Biotransformation by hepatic $P450_{IB}$ (CYP2C) controls mefenamic acid elimination. Clin Pharmacol Therap 1994; 55: 139.
39. Miners JO, Coulter S, Tukey RH, Veronese ME, Birkett DJ. Cytochromes P450 1A2 and 2C9 are responsible for the human hepatic O-demethylation of R- and S-naproxen. Biochem Pharmacol 1996; 51: 1003-1008.
40. Weaver RJ, Dickins M, Burke MD. Cytochrome P4502C9 is responsible for hydroxylation of the naphthoquinone antimalarial drug 58C80 in human liver. Biochem Pharmacol 1993; 46: 1183-1197.
41. Leeman TD, Transon C, Bonnabry P, Dayer P. A major role for cytochrome $P450_{IB}$ (CYP2C subfamily) in the actions of non-steroidal anti-inflammatory drugs. Drugs Exp Clin Res 1993; 19: 189-195.
42. Stearns RA, Chakravarty PK, Chen R, Lee Chiu S-H. Biotransformation of losartan to its active carboxylic acid metabolite in human liver microsomes. Drug Metab Dispos 1995; 23: 207-215.
43. Andersson T, Miners JO, Veronese ME, Tassaneeyakul W, Tassaneeyakul W, Meyer UA, Birkett DJ. Identification of human liver cytochrome P450 isoforms mediating omeprazole metabolism. Br J Clin Pharmacol 1993; 36: 521-530.
44. Hall SD, Guengerich FP, Branch RA, Wilkinson GR. Characterization and inhibition of mephenytoin 4-hydroxylase activity in human liver microsomes. J Pharmacol Exp Ther 1987; 240: 216-222.
45. Birkett DJ, Rees D, Andersson T, Gonzalez FJ, Miners JO, Veronese ME. In vitro proguanil activation to cycloguanil by human liver microsomes is mediated by CYP3A isoforms as well as by 3-mephenytoin hydroxylase. Br J Clin Pharmacol 1994; 37: 413-420.
46. McGinnity DF, Griffin SJ, Moody GC, Voice M, Hanlon S, Friedberg T, Riley RJ. Rapid characterization of the major drug-metabolizing human hepatic cytochrome P450 enzymes expressed in *Escherichia coli*. Drug Metab Dispos 1999; 27: 1017-1023.
47. Bajpai M, Roskos LK, Shen DD, Levy RH. Roles of cytochrome P4502C9 and cytochrome P4502C19 in the stereoselective metabolism of phenytoin to its major metabolite. Drug Metab Dispos 1996; 24: 1401-1403.
48. Knodell RG, Dubey RK, Wilkinson GR, Guengerich FP. Oxidative metabolism of hexobarbital in human liver: relationship to polymorphic S-mephenytoin oxidation. J Pharmacol Exp Ther 1988; 245: 845-849.
49. Kobayashi K, Kogo M, Tani M, Shimada N, Ishizaki T, Numazawa S, Yoshida T, Yamamoto T, Kuroiwa Y, Chiba K. Role of CYP2C19 in stereoselective hydroxylation of mephobarbital by human liver microsomes. Drug Metab Dispos 2001; 29: 36-40.
50. Hoskins J, Shenfield G, Murray M, Gross A. Characterization of moclobemide N-oxidation in human liver microsomes. Xenobiotica 2001; 31: 387-397.
51. Facciola G, Hidestrand M, von Bahr C, Tybring G. Cytochrome P450 isoforms involved in melatonin metabolism in human liver microsomes. Eur J Clin Pharmacol 2001; 56: 881-888.

52. VandenBranden M, Ring BJ, Binkley SN, Wrighton SA. Interaction of human liver cytochromes P450 in vitro with LY307640, a gastric proton pump inhibitor. Pharmacogenetics 1996; 6: 81-91.
53. Yamazaki S, Sato K, Suhaka K, Sakaguchi M, Mihara K, Omura T. Importance of the proline-rich region following signal-anchor sequence in the formation of correct conformation of microsomal cytochrome P450s. J Biochem 1993; 114: 652-657.
54. Chen C-D, Kemper B. Different structural requirements at specific proline residue positions in the conserved proline-rich region of cytochrome P450 2C2. J Biol Chem 1996; 271: 28607-28611.
55. Ridderström M, Masimirembara C, Trump-Kallmeyer S, Ahlefelt M, Otter C, Andersson TB. Arginines 97 and 108 in CYP2C9 are important determinants of the catalytic function. Biochem Biophys Res Commun 2000; 270: 983-987.
56. Straub P, Lloyd M, Johnson EF, Kemper B. Cassette mutagenesis of a potential substrate recognition region of cytochrome P450 2C2. J Biol Chem 1993; 268: 21997-22003.
57. Richardson TH, Johnson EF. Alterations of the regiospecificity of progesterone metabolism by the mutagenesis of two key amino acid residues in rabbit cytochrome P450 2C3v. J Biol Chem 1994; 269: 23927-23943.
58. Tracy TS, Hutzler JM, Haining RL, Rettie AE, Hummel MA, Dickmann LJ. Polymorphic variants (CYP2C9*3 and CYP2C9*5) and the F114L active site mutation of CYP2C9: effect on atypical kinetic metabolism profiles. Drug Metab Dispos 2002; 30: 385-390.
59. Kronbach T, Larabee TM, Johnson EF. Hybrid cytochromes P450 identify a substrate binding domain in P450IIC5 and P450IIC4. Proc Natl Acad Sci USA 1989; 86: 8262-8265.
60. Kaminsky LS, de Morais SMF, Faletto MB, Dunbar DA, Goldstein JA. Correlation of human cytochrome P4502C substrate specificities with primary structure: warfarin as a probe. Mol Pharmacol 1993; 43: 234-239.
61. Hsu M-H, Griffin KJ, Wang Y, Kemper B, Johnson EF. A single amino acid substitution confers progesterone 6-hydroxylase activity to rabbit cytochrome P450 2C3. J Biol Chem 1993; 268: 6939-6944.
62. Faletto MB, Linko P, Goldstein JA. A single amino acid mutation $Ser^{180}Cys$ determines the polymorphism in cytochrome P450g (P4502C13) by altering protein stability. J Biol Chem 1992; 267: 2032-2037.
63. Jung F, Griffin KJ, Song W, Richardson TH, Yang M, Johnson EF. Identification of amino acid substitutions that confer a high affinity for sulfaphenazole binding and a high catalytic efficiency for warfarin metabolism to P450 2C19. Biochemistry 1998; 37: 16270-16279.
64. Ohgiya S, Komori M, Ohi H, Shiramatsu K, Shinriki N, Kamataki T. Six-base deletion occurring in messages of human cytochrome P450 in the CYP2C subfamily results in reduction of tolbutamide hydroxylase activity. Biochem Int 1992; 27: 1073-1081.
65. Klose TS, Ibeanu GC, Ghanayem BI, Pedersen LG, Li L, Hall SD, Goldstein JA. Identification of residues 286 and 289 as critical for conferring substrate

specificity of human CYP2C9 for diclofenac and ibuprofen. Arch Biochem Biophys 1998; 357: 240-248.

66. Imai Y, Nakamura M. Point mutations at threonine-301 modify substrate specificity of rabbit liver microsomal cytochromes P450 laurate (ω-1)-hydroxylase and testosterone 16α-hydroxylase. Biochem Biophys Res Commun 1989; 158: 717-722.
69. Afzelius L, Zamora I, Ridderström M, Andersson TB, Karlen A, Masimirembwa CW. Competitive CYP2C9 inhibitors: enzyme inhibition studies, protein homology modeling and three-dimensional quantitative structure-activity relationship analysis. Mol Pharmacol 2001; 59: 909-919.
70. Ramarao MK, Straub P, Kemper B. Identification by in vitro mutagenesis of the interaction of two segments of C2MstC1, a chimera of cytochromes P450 2C2 and P450 2C1. J Biol Chem 1995; 270: 1873-1880.
71. Veronese ME, Doecke CJ, Mackenzie PI, McManus ME, Miners JO, Rees DLP, Gasser R, Meyer UA, Birkett DJ. Site-directed mutation studies of human liver cytochrome P450 enzymes in the CYP2C subfamily. Biochem J 1993; 289: 533-538.
72. Uno T, Imai Y, Nakamura M, Okamoto N, Fukuda T. Importance of successive prolines in the carboxy-terminal region of P450 2C2 and P450 2C14 for the hydroxylase activities. J Biochem 1993; 114: 363-369.
73. Von Wachenfeldt C, Johnson EF. Structures of eukaryotic cytochrome P450 enzymes. In: Ortiz de Montellano PR,, ed. Cytochrome P450. New York: Plenum Press, 1995; 183-223.
74. Gotoh O. Substrate recognition sites in cytochrome P450 family 2 (CYP2) proteins inferred from comparative analysis of amino acid and coding nucleotide sequences. J Biol Chem 1992; 267: 83-90.
75. Lewis DFV, Bailey PT, Low LK. Molecular modelling of the mouse cytochrome P450 CYP2F2 based on the CYP102 crystal structure template and selective CYP2F2 substrate interactions. Drug Metab Drug Interact 2002; 19: 97-113.
76. Lewis DFV, Lake BG, Dickins M, Goldfarb PS. Molecular modelling of CYP2B6 based on homology with the CYP2C5 crystal structure: analysis of enzyme-substrate interactions. Drug Metab Drug Interact 2002; 19: 115-135.